Multi-Conjugate Adaptive Optics: a PSF study
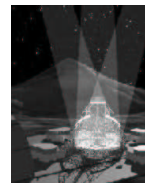
Miska Le Louarn

Center for Adaptive Optics, UCSC Kerr Hall, Santa Cruz CA, USA

ABSTRACT

A model of a multi-conjugate adaptive optics system is used to estimate the performance of such a system in the infrared and in the visible. It is shown that the corrected field of view can be largely increased, using a Gemini-like system. Residual anisoplanatism is studied, when different natural guide star schemes are used. In any case the field of view is significantly increased. A scheme to increase this field even more, at the expense of Strehl ratio stability is presented. It is also noted that very high angular resolution ($\sim$20 milli-arcsec) can be obtained over a 70 arcsec (diameter) field of view, even if this system is designed for IR use.

1. INTRODUCTION

In this paper, the results of a Multi-conjugate adaptive optics (MCAO) system are presented. A Gemini like system is presented, including 5 laser guide stars (LGSs) and shack-Hartmann (SH) wavefront sensors, and 3 deformable mirrors (DMs). The lower order modes are measured through 1 Natural guide star (NGS) and a 3x3 SH sensor or with 3 NGSs placed in the corrected field of view (FOV), measured by a quad-cell type detector. The simulation is done in closed-loop, including temporal evolution. The results are described in terms of Strehl ratio and full-width at half maximum (FWHM) of the point spread function (PSF).

In the first section, the model is described and the hardware parameters are summarized. The second section presents the results in the infrared, for which the system is designed for, in terms of sub-aperture size and number of actuators. In the following section, its behavior in the visible is computed and analyzed. Finally, the conclusions are presented.

2. AO SIMULATION MODEL

The AO system is modeled using a complex end to end simulation tool, which shall be described more in detail in a forthcoming paper.

The atmosphere is modeled with 7 infinitely thin phase screens, generated with the algorithm presented by Mcglamery, 1976. Therefore, these screen are circular, i.e. they can be wrapped around as they are shifted to create temporal evolution. This production method creates an ad-hoc outer scale of turbulence of $\sim$ 30 m, compatible with recent measurements (Martin et al., 2000). The turbulence characteristics are the same as in the Gemini simulations (Ellerbroek and Rigaut 2000, Ellerbroek and Rigaut 2001). These phase screens are shifted and magnified to produce the effect of off-axis guide stars and LGSs, respectively. LGSs are placed at a constant height of 90 km above the telescope. The screens are then summed (geometric optics) and the sum is sent to the wavefront sensor module.

The wavefront sensors module take the phase screen created as described in the previous section and cut it into small sub-aperture sized square pieces. The PSF in each sub-aperture is computed using a fast Fourier transform. Then these PSFs are re-sampled to take into account the pixelelization of the WFS detector, a CCD. Finally, photon, read-out and dark current noise are added to the images. Then the centroid is computed and this forms the measurement of a sub-aperture. Throughout this paper, it is assumed that both LGSs and NGSs are bright, and therefore the photon noise is the dominant source of error. The wavefront sensor module is adapted from the European Training and Mobility of Researchers (TMR) for "laser guide stars on 8-m telescopes" simulation tool, LA3OS2 (Carbillet et al. 1999).

Further author information: (Send correspondence to MLL)
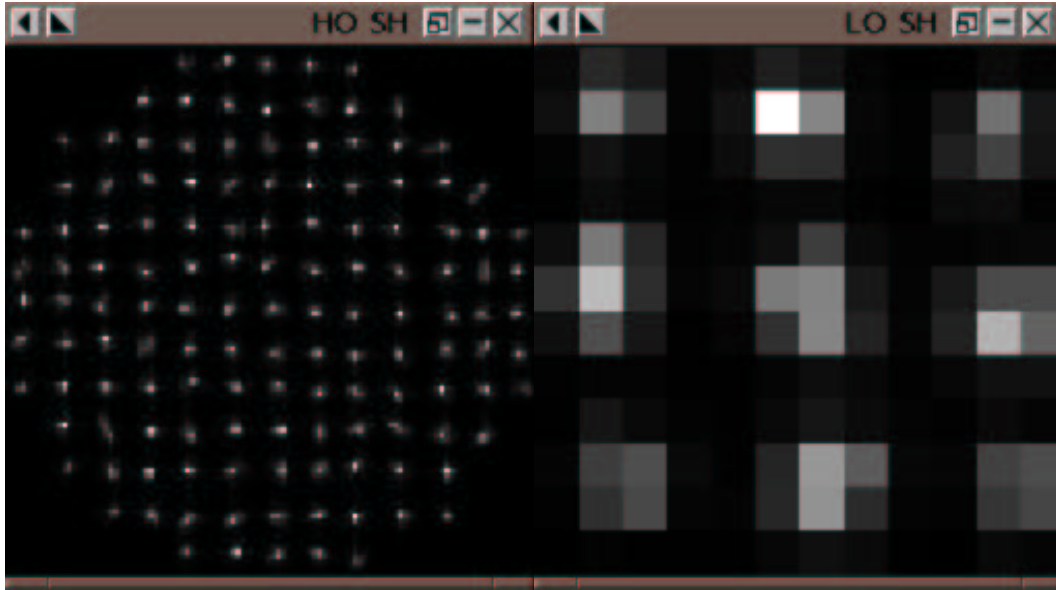
MLL: E-mail: lelouarn@ucolick.org

Figure 1. Images of the SH wavefront sensors, as produced by the simulation. The left hand-side on is a high order WFS observing an LGS, the right hand side one is a low order WFS observing a NGS. Notice the speckle structures in the WFS since the wavefront sensing is done at visible wavelengths.
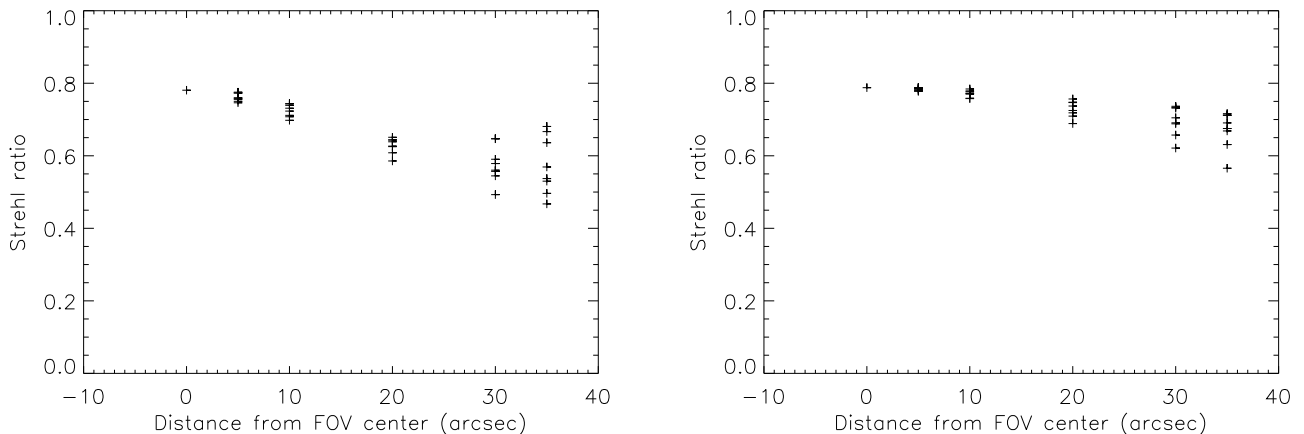

Figure 2. Strehl ratios as a function of field angle for the SVD control algorithm (left) and the MAP control algorithm (right), after 100 iterations (i.e. 200 ms), in the K band. Notice how the Strehl ratios are consistently higher with the MAP approach, and how the spread in Strehl at different position angles is reduced.

This procedure is repeated for each sub-aperture and each guide star, and the wavefront slopes are concatenated into a single measurement vector, containing a number of slopes equal to the number of guide stars times the total number of sub-apertures.

The system interaction matrix is constructed as described in , Le Louarn and Tallon, 2001. This interaction matrix can be used (using an SVD inversion) to control the MCAO system. However, a more sophisticate approach, based on a Maximum a Posteriori (MAP) approach is used, since it produces better results (Fusco et al. 1999), as shown on Fig. 2. The algorithm is a linear operation applied to the measured slopes, producing commands to be sent to the 3 DMs, which are optically conjugated to 0.0, 4.5 and 9.0 km, as in the Gemini system. The corrected field of view (FOV) is 30 arcsec in radius. The DMs are sized accordingly.

This system is run in closed loop by injecting the corrected phase as a new measurement to the wavefront sensor. In order to take into account the slow decorrelation time of the low-order modes, the simulation is run for 2000 iterations, corresponding to 10 s in real life. It was verified that if the low order modes are not measured, the performance of the system is significantly reduced and therefore these modes a modeled properly.
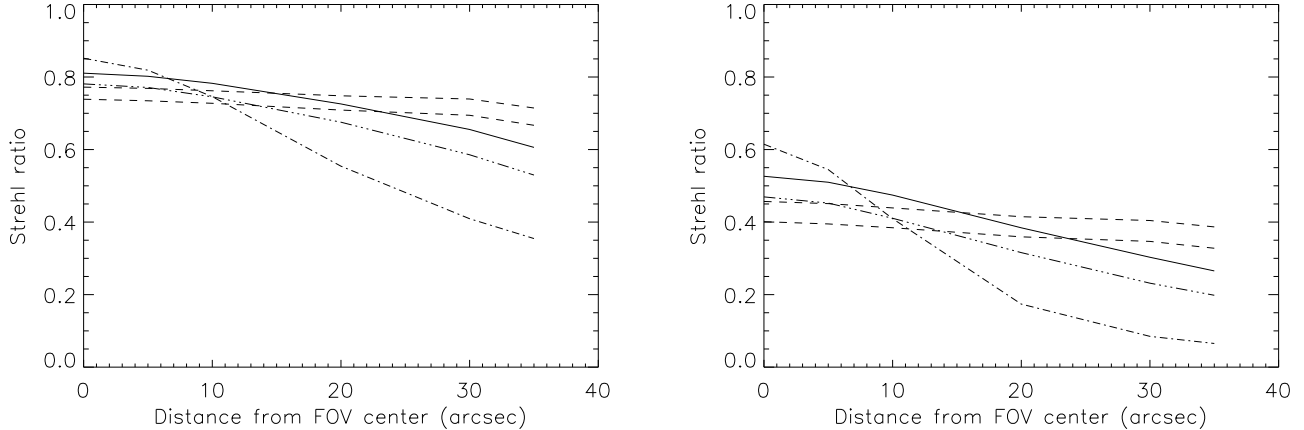
Figure 3. Strehl ratio as a function of field angle for three AO systems: a conventional NGS AO system (dot-dash), a 1 NGS MCAO system (solid) and a 3 NGS MCAO system (dash, the top curve being with 28 arcsec NGS separation, the lower one for 42 arcsec), for two wavelengths, K band (left) and J band (right). The 3 NGS with 14 arcsec NGS separation was omitted for clarity. It overlaps almost perfectly the 28 arcsec 3NGS curve. The triple-dash dot curve corresponds to the case where only tipt-tilt is measured from the single central guide star.

All results presented here are made at zenith, with a Fried parameter of r_0 of 20 cm (at 0.5 μm).

3. SIMULATION RESULTS IN THE IR

Three AO systems are considered. A conventional NGS AO system, using a single wavefront sensor (same number of sub-apertures as a LGS WFS in the MCAO system), an MCAO system using 1 NGS (called 1NGS system) and a system using 3 NGSs placed in the corrected field of view, called the 3NGS system. Three different NGS configurations are used in that system, where the 3 NGS are placed at radii of 42, 28 and 14 arcsec from the center, in a triangular configuration. The first point represents an extreme case, since the stars are already slightly outside the corrected FOV (30 arcsec in radius). Each point is the average of 6 Strehl ratios, observed at 6 "probe stars" observed at different position angles in the corrected FOV.

On Fig. 3, the Strehl as a function of field angle is plotted, for two wavelengths (K and J), for the different AO systems. The NGS AO systems is used to shown the improvement brought in field stability by the MCAO systems. It can be seen that anisoplanatism reduces the Strehl significantly, even in the K band, since it drops from 0.85 to 0.35 over the 35 arcsec probed field. For the MCAO case, the Strehl drops slightly for the 1NGS case (from 0.83 to 0.6) and the stability is even better with the 3NGS system, since the Strehl is almost constant at 0.77. Slight anisoplanatism begins to appear, as expected, outside the deformable mirror (at distances beyond 30 arcsec, the nominal corrected FOV). It should be noted that the position of the 3NGS is not very critical within the studied range, the most significant effect appearing when they are outside the corrected FOV. Of course, if they are too close to one-another, anisoplanatism will appear. In that case, the performance will tend to the case where only tilt is corrected. That case is also shown on Fig. 3.

An interesting effect appears when one wants to observe beyond the field corrected by the deformable mirrors (see Fig 4). Indeed, part of the phase coming from the object is corrected, while another part is uncorrected atmospheric turbulence. Therefore, residual anisoplanatism will appear, but not as severely as in conventional AO, since some parts are still corrected. This is demonstrated on Fig. 5. The Strehl (in K band) as a function of field angle is plotted. This plot takes only into account one direction and not 6 different probe stars at different position angles, hence the slight difference with Fig. 3. It can be seen that the Strehl ratio slowly rolls off after the vertical bar, indicating the edge of the DM. The Strehl ratio of the MCAO system achieves the Strehl ratio obtained with the NGS AO system at 30 arcsec at 57 arcseconds (radius), in the K band. The brake due to the edge of the DM is clearly seen. This approach of letting some uncorrected phase be taken into account seems to work as expected, allowing one to furthermore increase the corrected FOV without increasing the DM size (i.e. system complexity). Another method would be to mask out the photons coming from outside of the DM.
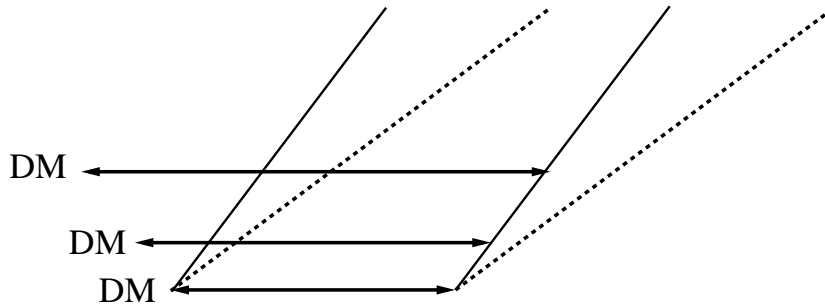
Figure 4. The DMs (arrows) limit the corrected FOV (solid lines). If a larger angle is observed (dashed lines) some uncorrected turbulence will appear. However, a part is still corrected (especially the ground turbulence) and the performance does not drop as sharply as with conventional anisoplanatism.
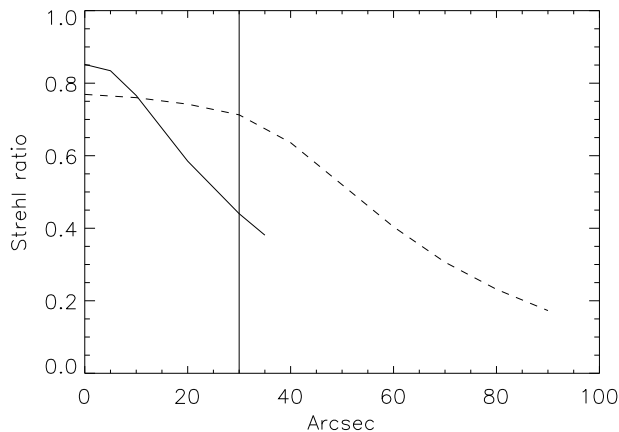

Figure 5. Anisoplanatic behavior when one observes "outside" of the corrected FOV. Only the first 3 arcsec are covered by the DMs. The solid line is the conventional NGS AO system, the dashed line is the 3NGS (28 arcsec) system. After 30 arcsec, only a part of the wavefront is corrected.

This has the advantage of not reducing the Strehl ratio. However, the flux from these objects is then reduced by vignetting.

The choice between the two approaches must obviously be made by considering the astrophysical problem: an integral field spectrometer, for example, will benefit from the light concentration brought by the AO system, and will not be very sensitive to the loss in Strehl ratio. However, a loss in flux due to vignetting will significantly increase the integration time, a critical parameter in imaging of faint objects.

4. SIMULATION RESULTS IN THE VISIBLE

Although these AO systems are designed to give optimum performance in the IR, it is well known that a significant performance gain can still be obtained in the visible, if good seeing conditions are present and observations near zenith are done.

To investigate this phenomenon in MCAO systems, PSFs are computed in the V band (0.55 μm). The results are shown on Fig. 7. Both Strehl ratios and FWHM are plotted, as measured from the simulated PSFs. No analytic approximation to the FWHM has been used. These figures show that the Strehl ratios are low for all systems, since aliasing and fitting errors are large. The maximum Strehl ratio is obtained on-axis with the NGS-AO system, 0.09. However anisoplanatism rapidly reduces Strehl, and at 20 arcsec, it is only 0.003. On the other hand, MCAO systems have an almost constant Strehl ratio, since for the 3NGS system, it ranges only from 0.025 (center) to 0.015 (at 35 arcsec). Although low, these Strehl ratios still show interesting properties, as shown by the FWHM. On the NGS-AO system, it ranges from 0.016 arcsec (center) to 0.212 (35 arcsec), a significant degradation indeed. The MCAO system on the other hand shows very little evolution in the field, since the FWHM varies from 0.022 to 0.025. Therefore, very high resolution imaging is available on large FOVs
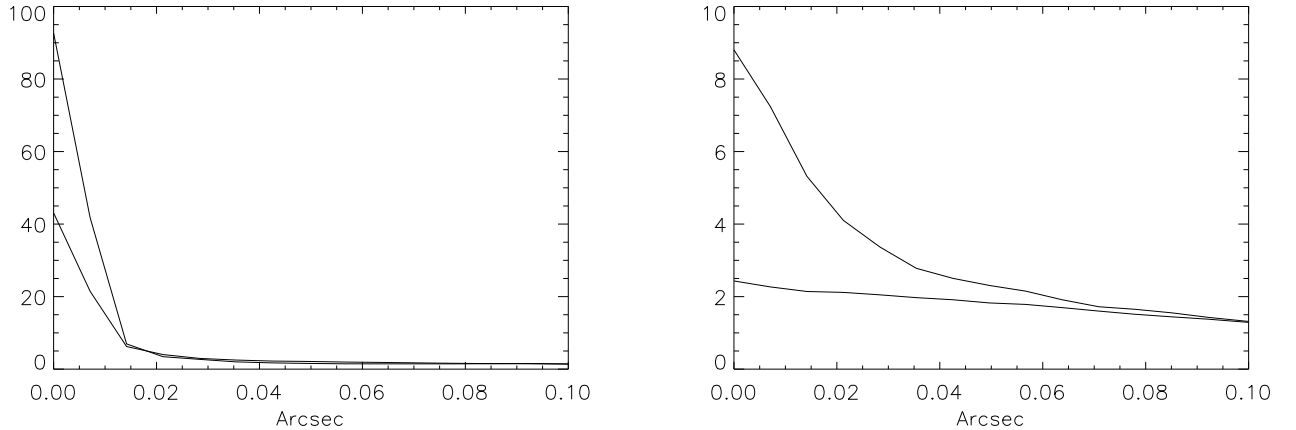
4

Figure 6. Radial average PSF profiles, for on-axis PSFs (left) and 35 arcsec off-axis (right). Two AO systems are represented: The NGS-AO system (top curve on the left, bottom curve on the right figure) and the MCAO system with 3 NGS at 28 arcsec.

(over 70 arcsec in diameter) in the visible, an extremely significant improvement over conventional AO systems. It is surprising at first sight that such good performance can be seen and that residual anisoplanatism does not appear. However, it has been shown (Tokovinin et al. 2001) that the limiting factor in such an MCAO configuration is beam overlap and not the intermediate turbulent layers. Moreover, the PSF behavior is different in an MCAO system: the low order modes (measured from the NGS) contribute significantly to anisoplanatism (as shown by the difference in field stability between the 3NGS at different angles and the 1NGS methods). However, the FWHM is less sensitive to the low order mode errors as is the case for single LGS PSF when tilt is poorly measured. Indeed, as shown by Rigaut et al. (1998) and Le Louarn et al. (1998), when tip-tilt is not well corrected, the well corrected short exposure PSF is jittered. This reduces the Strehl ratio, but the FWHM (or the encircled energy) change by small amounts, since the energy does not go into a large halo as in conventional AO. A similar phenomenon is seen here, for the first time, in MCAO.

The difference in PSF shape evolution can be seen on Fig 6. It shows the radial averaged profile of the NGS-AO PSF and the MCAO PSF, for the on-axis and off-axis case. The MCAO case clearly shows that the PSF is not diffaction limited (off-axis), but there is no large halo. The FWHM has increased from the diffraction limited case, but still has a FWHM a roughly 20 mas. The diffraction limit at 0.55 μm is 14.1 mas.

Therefore, it is suggested, that a large field of view visible camera be a part of the instrumentation of an MCAO system designed for the IR. For example, high angular resolution imaging of planets (Jupiter is ~ 40 arcsec in diameter), globular clusters, galactic and AGN nuclei would greatly benefit from such an instrument. It should be noted that the 20 mas resolution is 5 times better that the HST planetary camera(PC), if the limited sampling is taken into account.

5. CONCLUSIONS

In this paper, simulations of an MCAO system, designed to work in the visible are presented. It is shown that 3 DMs allow to significantly increase the corrected FOV. No significant anisoplanatism is seen over a 30 arcsec (radius) diameter, when 3 NGSs are used. When only 1 NGS is used, anisoplanatism appears, but slightly higher Strehl ratios in the center of the FOV are observed. Moreover, a scheme to increase the FOV even more, at the expense of FOV stability is presented. This could be useful for example on integral field spectrographs, where energy consentration is more important than the highest angular resolution and field stability.

A remarkable property of MCAO systems is then presened, i.e. its ability to provide a high angular resolution over a wide FOV, even if Strehl ratios are low (a percent, or so). This could have a significant impact on the instrumentation of future MCAO systems, which could include a visible light high angular resolution camera, even if the system is designed for visible light operation.
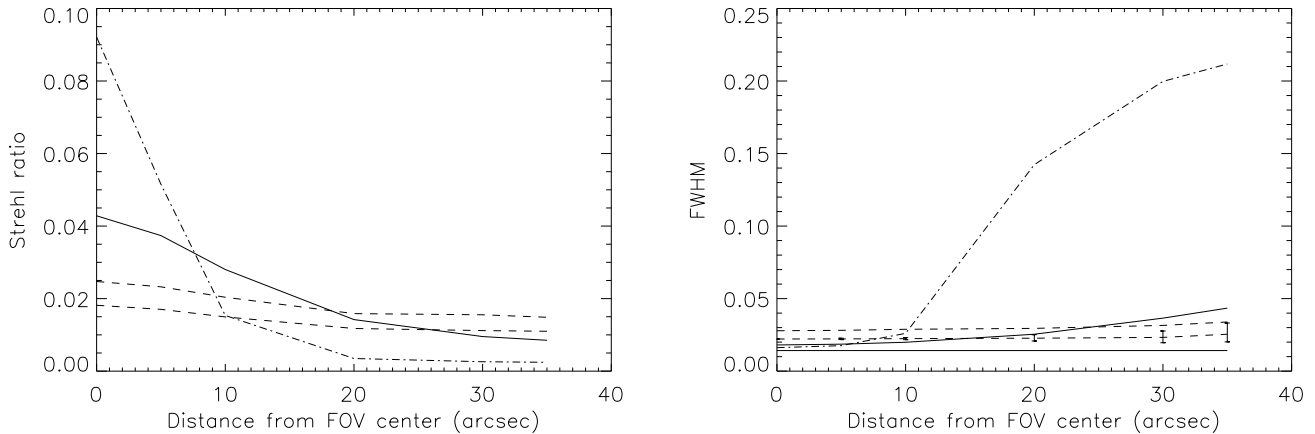
Figure 7. Strehl as a function of distance from the FOV center in the V band (left) for the three AO systems. On the right, the Full Width at Half Maximum of the PSF for the same systems, also in V. Notice how the FWHM of the NGS-AO system increases when the MCAO systems show a quasi-constant FWHM.

REFERENCES

Carbillet et al., 1999 Carbillet, M., Femenia, B., Delplancke, F., Esposito, S., Fini, L., Riccardi, A., Viard, E., Hubin, N. N., and Rigaut, F. J. (1999). La3os2: a software package for laser guide star adaptive optics systems. *Proc. SPIE*, 3762:378–389.

Ellerbroek and Rigaut, 2001 Ellerbroek, B. L. and Rigaut, F. (2001). Methods for correcting tilt anisoplanatism in laser-guide-star-based multi-conjugate adaptive optics. *J. Opt. Soc. Am. A*, submitted.

Ellerbroek and Rigaut, 2000 Ellerbroek, B. L. and Rigaut, F. J. (2000). Scaling multiconjugate adaptive optics performance estimates to extremely large telescopes. In Wizinowich, P. L., editor, *Adaptive Optical Systems Technology*, volume 4007 of *SPIE Conference*, pages 1088–1099. Society of Photo-Optical Instrumentation Engineers, Bellingham, WA.

Fusco et al., 1999 Fusco, T., Conan, J.-M., Michau, V., Mugnier, L. M., and Rousset, G. (1999). Phase estimation for large field of view: application to multiconjugate adaptive optics. *Proc. SPIE*, 3763:125–133.

Le Louarn et al., 1998 Le Louarn, M., Hubin, N., Foy, R., and Tallon, M. (1998). Sky coverage and psf shape with lgs ao on 8 m telescopes. *Proc. SPIE*, 3353:364–370.

Le Louarn and Tallon, 2000 Le Louarn, M. and Tallon, M. (2000). Analysis of the modes and behaviour of a multiconjugate adaptive optics system. *J. Opt. Soc. Am. A*, submitted.

Martin et al., 2000 Martin, F., Conan, R., Tokovinin, A., Ziad, A., Trinquet, H., Borgnino, J., Agabi, A., and Sarazin, M. (2000). Optical parameters relevant for high angular resolution at paranal from gsm instrument and surface layer contribution. *A&AS*, 144:39–44.

McGlamery, 1976 McGlamery, B. L. (1976). Computer simulation studies of compensation of turbulence degraded images. *Proc. SPIE*, 74:225–233.

Rigaut et al., 1998 Rigaut, F., Bonaccini, D., and Monnet, G. (1998). *Laser Guide Star adaptive optics for astronomy*. NATO ASI - Kluwer academic press.

Tokovinin et al. 2001, 2000 Tokovinin, A., Le Louarn, M., Viard, E., and Conan, R. (2001). *A&A*, submitted.